Controlled Pseudopod Extension of Human Neutrophils Stimulated with Different Chemoattractants

Doncho V. Zhelev,* Abdullatif M. Alteraifi,† and David Chodniewicz*
*Department of Mechanical Engineering and Materials Science, Duke University, Durham, North Carolina 27708-0300 USA; and
†Department of Mechanical Engineering, United Arab Emirates University, Al Ain, United Arab Emirates

ABSTRACT The formation of pseudopods and lamellae after ligation of chemoattractant sensitive G-protein coupled receptors (GPCRs) is essential for chemotaxis. Here, pseudopod extension was stimulated with chemoattractant delivered from a micropipet. The chemoattractant diffusion and convection mass transport were considered, and it is shown that when the delivery of chemoattractant was limited by diffusion there was a strong chemoattractant gradient along the cell surface. The diffusion-limited delivery of chemoattractant from a micropipet allowed for maintaining an almost constant chemoattractant concentration at the leading edge of single pseudopods during their growth. In these conditions, the rate of pseudopod extension was dependent on the concentration of chemoattractant in the pipet delivering chemoattractant. The pseudopod extension induced using micropipets was oscillatory even in the presence of a constant delivery of chemoattractant. This oscillatory pseudopod extension was controlled by activated RhoA and its downstream effector kinase ROCK and was abolished after the inhibition of RhoA activation with *Clostridium botulinium* C3 exoenzyme (C3) or the blocking of ROCK activation with Y-27632. The ability of the micropipet assay to establish a well-defined chemoattractant distribution around the activated cell over a wide range of molecular weights of the used chemoattractants allowed for comparison of the effect of chemoattractant stimulation on the dynamics of pseudopod growth. Pseudopod growth was stimulated using *N*-formylated peptide (*N*-formyl-methionyl-leucyl-phenylalanine (fMLP)), platelet activating factor (PAF), leukotriene B4 (LTB_4), C5a anaphylotoxin (C5a), and interleukin-8 (IL-8), which represent the typical ligands for G-protein coupled chemotactic receptors. The dependence of the rate of pseudopod extension on the concentration of these chemoattractants and their equimolar mixture was measured and shown to be similar for all chemoattractants. The inhibition of the activity of phosphoinositide-3 kinase (PI3K) with wortmannin showed that 72%–80% of the rate of pseudopod extension induced with *N*-formyl-methionyl-leucyl-phenylalanine, platelet activating factor, and leukotriene B4 was phosphoinositide-3 kinase-dependent, in contrast to 55% of the rate of pseudopod extension induced with interleukin-8. The dependence of the rate of pseudopod extension on the concentration of individual chemoattractants and their equimolar mixture suggests that there is a common rate-limiting mechanism for the polymerization of cytoskeletal F-actin in the pseudopod region induced by G-protein coupled chemoattractant receptors.

INTRODUCTION

Human neutrophils are part of the innate immune system, where their main function is to extravasate from the microvasculature and migrate toward sites of inflammation where they kill invading bacteria and other pathogens by either phagocytosis or a release of superoxide products and/or proteolytic enzymes (Luster, 1998; Tessier et al., 1997; Zhang et al., 2001). Neutrophils also play an important role in hematopoiesis, where they are involved in the mobilization of hematopoietic progenitor/stem cells (HPCs) (Cottler-Fox et al., 2003; Martin et al., 2003; Papayannopoulou, 2004). Chemotaxis is critical for these functions, which is evident from the involvement of chemotactic receptors in both immune responses and hematopoiesis. For example, the chemokine receptors CXCR1 and CXCR2, as well as the leukotriene receptors, are critical for the control of extravasation and migration through tissue (Luster, 1998; Tessier et al., 1997; Zhang et al., 2001), whereas receptors for end-target chemoattractants, such as the *N*-formylated peptide and complement anaphylotoxin receptors, regulate neutrophil responses at sites of inflammation (Heit et al., 2002; Katanaev, 2001). Similarly, hematopoiesis requires neutrophil chemotaxis to the bone marrow, where the homing of mature neutrophils (Martin et al., 2003) is necessary for the secretion of metalloproteinase 9 (MMP-9) during the chemokine-dependent mobilization of hematopoietic progenitor/stem cells (Pruijt et al., 2002; Papayannopoulou, 2004). Neutrophil homing as well as the homing of other white blood cells is controlled by the chemokine receptor CXCR4 and its ligand stromal cell derived factor-1α (SDF-1α) secreted by stromal cells (Juarez and Bendall, 2004).

Neutrophil chemotaxis is closely regulated by a group of receptors loosely divided into two main groups called nonclassical and classical chemotactic receptors (Katanaev, 2001). The nonclassical receptors induce chemotaxis but do not induce degranulation and superoxide production. These include the tumor necrosis factor receptors (CD120a and

Submitted October 31, 2003, and accepted for publication March 29, 2004.

Address reprint requests to Doncho V. Zhelev, Dept. of Mechanical Engineering and Materials Science, Duke University, Durham, NC 27708-0300. Tel.: 919-660-5335; Fax: 919-660-8963; E-mail: dvzh@duke.edu.

David Chodniewicz's present address is Dept. of Immunology, The Scripps Research Institute, La Jolla, CA 92037.

0006-3495/04/07/688/08 $2.00

doi: 10.1529/biophysj.103.036699

CD120b), the platelet derived growth factor receptor, and the receptor for transforming growth factor β (Katanaev, 2001). The classical chemotactic receptors are G-protein coupled receptors (GPCRs) and are capable of inducing all immune functions of the neutrophil including chemotaxis, degranulation, and superoxide production. These receptors are divided into five groups named after their most common ligands, namely, the receptors for the *N*-formylated peptides, the receptor for the platelet activated factor (PAF), the chemokine receptors (CXCR1, CXCR2, and CXCR4), the complement anaphylotoxin receptors, and the leukotriene receptors (BLT1 and BLT2) (Tarlowe et al., 2003; Katanaev, 2001). It has been shown recently that the classical chemotactic receptors (called here also GPCRs) activate distinct pathways of intracellular signaling, which induce differential superoxide production and/or integrin activation (Nick et al., 1997; Berger et al., 2002). It has been shown also that GPCRs are intimately involved in the regulation of F-actin polymerization in the lamella region during chemotaxis, which is critical for cell crawling (Pollard et al., 2000; Katanaev, 2001). Different chemotactic receptors have different capacity to induce directional crawling (hierarchical chemotactic response), which is seen by the ability of these receptors to induce a stepwise crawling of neutrophils in complex chemoattractant gradients (Foxman et al., 1999; Heit et al., 2002). However, it is not known whether this differential intracellular signaling also induces F-actin polymerization in the lamella region with different rates.

The evidence for the differential intracellular signaling by GPCRs is derived mostly from studies of secretion or secretion-related responses (Berger et al., 2002; Haribabu et al., 2000), whereas the signaling of secretion and chemotaxis are known to follow distinct pathways of activation (Haribabu et al., 1999). Most importantly, chemotactic responses such as pseudopod extension were not desensitized after multiple exposures to chemoattractant (Alteraifi and Zhelev, 1997) in contrast to secretion responses (Haribabu et al., 2000). These differences suggest that, at least for pseudopod extension, the signaling of F-actin polymerization by different GPCRs may be limited to a degree of utilization of the recently identified phosphoinositide-3 kinase (PI3K)-dependent and -independent pathways of pseudopod growth (Chodniewicz and Zhelev, 2003a).

Here we model the distribution of chemoattractant in the micropipet assay for pseudopod extension (Zhelev et al., 1996) to define similar conditions for stimulating pseudopod growth with different chemoattractants. Then we use representative chemoattractants for the five classical chemotactic receptors and study the dependence of the rate of pseudopod extension on chemoattractant concentration. The used chemoattractants include *N*-formyl-methionyl-leucyl-phenylalanine (fMLP) for the *N*-formyl peptide receptors, PAF for PAFR, leukotriene B4 (LTB_4) for BLT1 and BLT2, C5a for complement anaphylotoxin receptors, and interleukin-8 (IL-8) for CXCR1 and CXCR2. To evaluate the utilization of the PI3K-dependent and -independent pathways of F-actin polymerization by different GPCRs we measured the decrease of the rate of pseudopod extension in the presence of wortmannin (WTM), which is a specific inhibitor of the activity of the PI3Ks of class I (Davies et al., 2000; Thelen et al., 1994; Wymann et al., 1996; Stoyanova et al., 1997). We also study the effect of blocking RhoA and ROCK activity on oscillatory pseudopod formation, which is observed during the stimulation of pseudopod growth in suspended cells.

MATERIALS AND METHODS

Numerical simulation

The numerical simulation of the distribution of chemoattractant around a spherical cell and a cell with a pseudopod was performed using the FIDAP fluid dynamics simulation package (Fluid Dynamics International, Evanston, IL).

Cell preparation

Human neutrophils were freshly isolated from whole blood obtained by venipuncture from consenting, healthy adult volunteers (mean age 29 $\pm$ 8.5 years) into vacutainers anticoagulated with K_2EDTA. The neutrophils were isolated by a one-step density gradient centrifugation on Polymorphoprep (Nycomed, Oslo, Norway), at 500 $\times$ *g* for 35 min at 23°C. The neutrophil fraction was washed once with Ca^{2+}/Mg^{2+}-containing Hanks' Balanced Salt Solution (HBSS), (Sigma Chemical, St. Louis, MO) and resuspended in an autologous plasma/HBSS solution (1:3, v/v). The cells were added to the manipulation chamber filled with an autologous plasma/HBSS solution (1:3, v/v). Microscopic evaluation of isolated cells indicated that 95% of the cells were neutrophils. The trypan blue dye exclusion test showed that >98% of the cells were viable. Approval for these studies was obtained from the Institutional Review Board at Duke University.

Micromanipulation

The experimental temperature controlled chamber was 2 mm thick. The bottom half of the chamber was covered with a cover glass strip and was open at both sides to allow for micromanipulation. The micropipets used to manipulate the cells were made from capillary glass tubing (A-M systems, Everett, WA) pulled with a vertical pipet puller (David Kopf Instruments, model 730, Tujunga, CA). The tip of the pipets was cut using a microforge. The micropipets were mounted on the microscope stage and inserted coaxially into the experimental chamber. They were connected to a manometer system, which allowed control of the pipet-chamber pressure difference. The temperature of the experimental chamber was controlled by flow of thermostated water and was measured with a thermocouple.

In the experiments of pseudopod extension, a single, passive neutrophil with smooth membrane surface and uniform optical density was chosen. The cell was held in a supporting pipet with a 5-μm internal diameter. Another pipet with an internal diameter of 1 μm was filled with a chemotactic solution of fMLP, PAF, LTB4, C5a, IL-8 (Sigma), or their equimolar mixture and positioned 1 μm from the cell surface. The used chemoattractants and inhibitors were initially diluted in either HBSS, or ethanol (with a maximal final concentration of 0.8%), or dimethyl sulfoxide (with a maximal final concentration of 0.2%). The following inhibitors were used: wortmannin (at 1-μM concentration and incubation for 15 min at 23°C; Sigma), *Clostridium botulinium* C3 exoenzyme (C3; 20-μg/ml concentration and incubation for 3 h at 23°C), and Y-27632 (10-μM concentration and incubation for 30 min at 23°C; Biomol, Plymouth Meeting, PA). The incubation of the cells with either ethanol or dimethyl sulfoxide at the above

concentrations had no measurable effect on the rates of pseudopod extension (data not shown).

Chemoattractant containing solution was blown over the cell, which initiated the extension of a single pseudopod. Pseudopod extension was observed using an inverted Nikon (Tokyo, Japan) microscope equipped with a 60× oil immersion objective. The microscope images were recorded using a charge-coupled device (CCD) camera (Cohu, San Diego, CA). A real-time counter and the chamber temperature were multiplexed onto the recorded images using a multiplexer (Vista Electronics, La Mesa, CA). The recorded images were analyzed with Metamorph Imaging software (Universal Imaging, Downingtown, PA), and the rate of pseudopod extension was calculated from the measured pseudopod lengths and time lapses. Approximately 90% of the neutrophils tested produced pseudopods. The nonresponding fraction of the cells was not reported in the averages of the rates of pseudopod extension.

Modeling the chemoattractant distribution

Pseudopod formation was stimulated using the assay shown in Fig. 3. Our previous use of this assay showed that the rate of pseudopod extension was dependent on the concentration of chemoattractant in the delivery pipet (Zhelev et al., 1996); however, the chemoattractant concentration at the leading edge of the extending pseudopod and the distribution of chemoattractant in the vicinity of the cell were not known. We used FIDAP to model the distribution of chemoattractant in the vicinity of the activated cell and to evaluate the concentration of chemoattractant at the leading pseudopod edge. In the micropipet assay, the chemoattractant was delivered using a small pipet as shown in Fig. 3, and the distribution of chemoattractant was dependent on both convection and diffusion. Two basic cell shapes were considered: a), a spherical shape representing the neutrophil before the start of pseudopod growth and b), a spherical shape with a single projection representing the neutrophil with a single pseudopod. The cell membrane was considered impermeable for chemoattractant.

The aqueous solution surrounding the cell was modeled as an incompressible Newtonian fluid. A small positive pressure was present in the pipet delivering chemoattractant, which induced flow of chemoattractant solution around the cell described by the continuity and the Navier-Stokes equations,

$$\nabla \cdot \vec{u} = 0, \tag{1}$$

$$\frac{\partial \vec{u}}{\partial t} + \vec{u} \cdot \nabla \vec{u} = -\nabla P + \frac{1}{R_e} \nabla^2 \vec{u}, \tag{2}$$

where $\vec{u}$ and P were the dimensionless velocity $\vec{u} = (u_z, u_r, u_\theta)$ and pressure respectively. R_e was the Reynolds number defined as $R_e = \rho U R_p / \mu$, where ρ was the fluid density, U was the characteristic velocity, R_p was the characteristic length, and μ was the fluid viscosity.

The chemoattractant released from the delivery pipet was also subject to diffusion, which was characterized by the diffusion equation,

$$\frac{\partial c_A}{\partial t} + \vec{u} \cdot \nabla c_A = \frac{1}{P_e} \nabla^2 c_A, \tag{3}$$

where c_A was the dimensionless chemoattractant concentration, $P_e = U R_p / D_{AB}$ was the Peclet number, and D_{AB} was the diffusion coefficient.

The dimensionless boundary conditions at the pipet orifice, cell surface, symmetry line, and the far stream were as follows (Fig. 1).

At the pipet orifice:

$$u_z = 1,\ u_r = 0,\ u_\theta = 0;\ \ and\ \ c_A = 1.$$

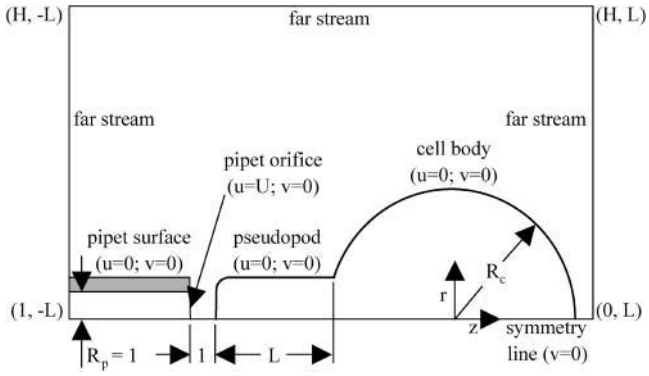

FIGURE 1 Schematics of the boundary conditions used in the numerical calculations.

At the cell surface:

$$u_z = 0,\ \ u_r = 0,\ \ u_\theta = 0\ \ (\text{no slip condition}),$$

$$j_A = -D_{AB} \left. \frac{\partial c_A}{\partial r} \right|_{\text{cell surface}} = 0\ \ (\text{impermeable membrane}).$$

At the symmetry line:

$$(r = 0, z):\ \ u_r = 0,\ \ \frac{\partial u_z}{\partial r} = 0,\ \ \frac{\partial c_A}{\partial r} = 0.$$

At the far stream:

$$\begin{aligned} (r, z = L \quad and \quad z = -L):&\quad \frac{\partial u_r}{\partial z} = \frac{\partial u_z}{\partial z} = 0, \quad c_A = 0, \\ (r = H, z):&\quad \frac{\partial u_r}{\partial z} = \frac{\partial u_z}{\partial z} = 0, \quad c_A = 0 \end{aligned}.$$

The parameters used in the model were determined as follows. The velocity of the fluid flow in the pipet was measured by tracking 0.2-μm latex beads or small liposomes made of the debris of red cell membranes (Zhelev and Needham, 1993). The calculated maximal fluid velocity at the center of the pipet for all experiments was on the order of 5 μm/s. The experimental solution for most experiments was made of 75% HBSS and 25% plasma. The viscosity of this solution was 1.17 cp, and its density was similar to the density of water (1 g/cm^3). The diffusion coefficient was inversely related to the molecular size by the Stokes-Einstein equation. The molecular mass of the used chemoattractant ranged from 0.3 to 0.4 kDa for LTB_4 and fMLP and from 8 to 11 kDa for IL-8 and C5a, respectively. The diffusion coefficient of *N*-formyl-norleucyl-leucyl-phenylalanine (FNLLP), which was similar to fMLP, was on the order of 10^{-5} cm^2/s (Stickle et al., 1984), and the diffusion coefficient of IL-8, which was the largest of the used chemoattractants, was on the order of 2.5×10^{-6} cm^2/s (Moghe et al., 1995). The chemoattractant distribution was calculated for diffusion coefficients from 10^{-5} to 10^{-6} cm^2/s (only the data for the diffusion coefficient equal to 10^{-6} cm^2/s are shown).

The FI-GEN module of FIDAP was used for mesh generation. The interior elements were four nodded quadrilaterals, whereas the boundary elements were two nodded linear elements. We used 1100 and 10,000 element mashes to test the dependence of the numerical solution on mesh density. The difference of the solutions for the two mesh densities did not

exceed 2%. The shown numerical solutions were for meshes with 1100 elements. The validity of the solutions was tested by introducing a residual vector error (0.001) and by testing for convergence. The transient solution reached convergence in less than 10 iterations. We also tested the validity of the solution by changing the domain size. The solutions for the domains extending from 50 to 100 μm from the cell surface were almost identical.

The modeling of the convective transport showed that even for low Reynolds numbers such as Reynolds numbers on the order of 5×10^{-5}, the streamlines of the liquid leaving the delivery pipet were strongly dependent on the cell shape (not shown). This suggested that at the regime of dominant convective mass transport (Peclet numbers larger than 1) the chemoattractant distribution around the cell would change with the change of the cell shape. To avoid experimental conditions, where chemoattractant distribution was dependent on cell shape, we worked in a regime of diffusion-limited mass transport by choosing low rates of chemoattractant delivery. The maximal rate of flow of chemoattractant from the delivery pipet in our experiments was on the order of 5 μm/s. The size of the neutrophil along the pseudopod axis in the presence of a maximally extended pseudopod was on the order of 15 μm, and the smallest diffusion coefficient for the chemoattractants used was 2×10^{-6} cm^2/s. For these values of the experimental parameters, the Peclet number was 0.4, which provided for diffusion-limited delivery of chemoattractant. The distribution of chemoattractant around the cell in these experimental conditions reached steady state within several seconds (data not shown). This was much smaller than the delay time for pseudopod extension measured experimentally (Fig. 3). The chemoattractant concentration at the leading edge of the pseudopod was strongly dependent on the distance between the cell and the delivery pipet, although it was independent of cell shape (Fig. 2). This provided conditions for steady-state stimulation of pseudopod extension at a constant concentration of chemoattractant at the leading edge of the extending pseudopod as long as the distance between the cell and the delivery pipet remained constant. The calculated chemoattractant concentration at the leading edge of the pseudopod decreased almost exponentially with the increase of the distance between the cell and the delivery pipet (not shown). For a distance between the cell and the delivery pipet equal to 1 μm, this decrease was 30%, which was the distance between the cell and the delivery pipet in our experiments. The diffusion-limited delivery of chemoattractant to the cell's surroundings was characterized by the generation of a steep chemoattractant gradient, where the chemoattractant concentration at the rare(back) of the cell was more than one order of magnitude smaller than the chemoattractant concentration at the leading edge (Fig. 2 *C*).

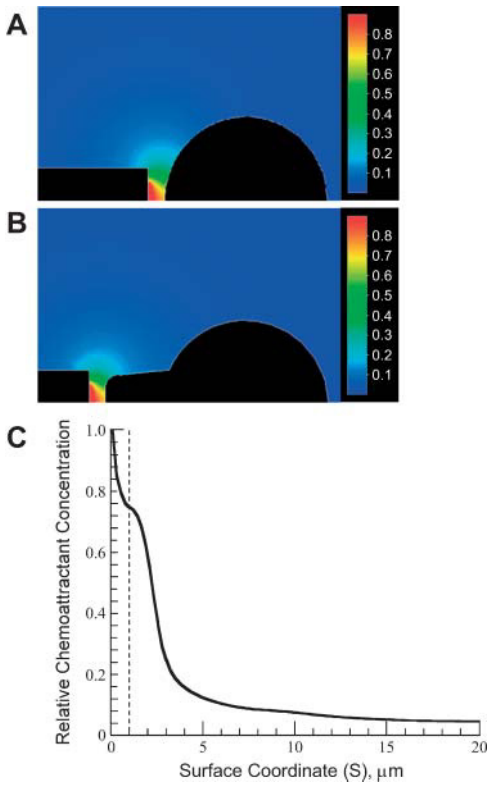

FIGURE 2 Dimensionless chemoattractant concentration for a spherical cell (*A*) and a cell with a 4-μm pseudopod (*B*). (*C*) Relative chemoattractant concentration verses the distance from the pipet orifice (*S* ordinate), which before reaching the cell surface is measured along the axes of symmetry and after reaching the cell surface is measured along the cell surface. The chemoattractant concentrations are scaled relative to the chemoattractant concentration in the delivery pipet. The concentration profiles for a spherical cell and for a cell with a 4-μm pseudopod are almost equivalent at steady state (the *two curves* are on top of each other). The dashed line marks the distance between the cell and the orifice of the delivery pipet.

EXPERIMENTAL RESULTS

Inducing pseudopod extension with the micropipet assay

The time course of the chemoattractant stimulated pseudopod extension in the micropipet assay is shown in Fig. 3. The distance between the cell and the delivery pipet was kept equal to 1 μm as the pseudopod length increased. This was done by retracting the pipet in front of the advancing pseudopod. During the retraction of the delivery pipet, there were small fluctuations of the distance between the cell and the pseudopod; however, these fluctuations did not produce measurable fluctuations of the rate of pseudopod extension. There was a delay from 10 to 15 s between the start of chemoattractant delivery and the beginning of the pseudopod growth (Fig. 3 *B*). This delay was attributed to the polymerization of noncytoskeleton F-actin by the neutrophil before the polymerization of the cytoskeletal F-actin, which supported the pseudopod shape. The polymerization of noncytoskeletal F-actin has been documented, and it has been shown to start immediately after the exposure of the cell to chemoattractant and peaks 10 s after activation (Niggli and Keller, 1997). The polymerization of the cytoskeleton F-actin, which is the focus of our study, starts ~10 s after activation (Niggli and Keller, 1997), which coincides with the beginning of pseudopod extension. The hallmark of the cytoskeleton F-actin is its sensitivity to treatment with wortmannin and its insolubility in Triton X-100 (Niggli and Keller, 1997).

After the beginning of pseudopod growth, the pseudopod length increased at almost constant rate for a period of 30–40 s (Fig. 3 *B*). This allowed the pseudopod to reach its maximal length. After reaching a maximal length, the pseudopod retracted and then increased its length and retracted it in an oscillatory fashion as long as the chemoattractant was delivered to the tip of the pseudopod. Fig. 1 *C* shows the change of pseudopod length verses time for a pseudopod stimulated with 10^{-7} M fMLP delivered with a pipet 1 μm

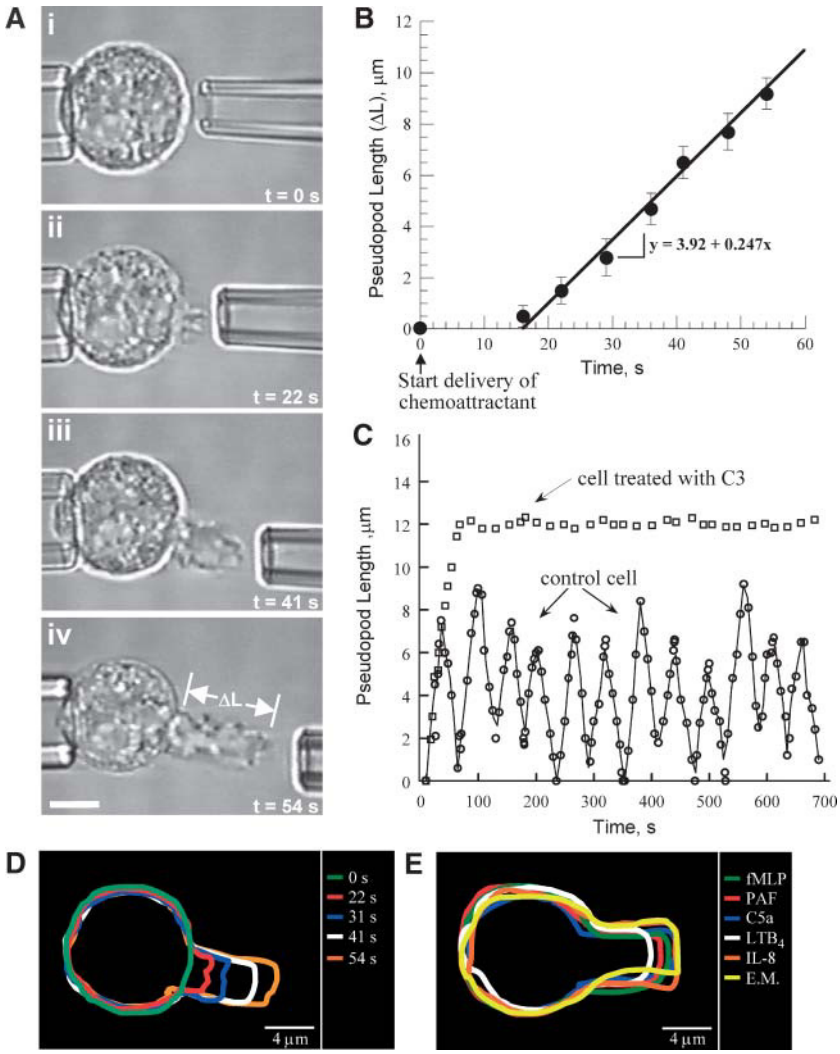

FIGURE 3 Pseudopod extension at 37°C. (*A*) A single passive neutrophil was held with a pipet in a gradient of chemoattractant established by the diffusion-limited delivery of chemoattractant from the delivery pipet. Before the beginning of the chemoattractant delivery, the cell was spherical (*i*). Immediately after the exposure of the cell to chemoattractant, its refractive index changed slightly (not shown), and 10–12 s later a single pseudopod started to grow (*ii*). The length of the pseudopod increased until a maximal length was reached (*iii* and *iv*), and then the pseudopod started to retract (not shown). The bar was 5 μm. (*B*) Time dependence of the increase of the length of the pseudopod during its initial growth. Pseudopod formation was stimulated with delivery of 10^{-7} M fMLP from a pipet as shown in *A*. The delivery of chemoattractant started at time 0. There was a delay of 10–12 s between the beginning of chemoattractant delivery and the beginning of pseudopod growth. After the beginning of the pseudopod growth, the length of the pseudopod increased almost linearly with the time until the maximal pseudopod length was reached. The slope of the dependence of the pseudopod length verses time was used for calculating the rate of pseudopod extension. (*C*) The continuous delivery of chemoattractant after the pseudopod has reached its maximal length resulted in an oscillatory pseudopod extension and retraction (○). This oscillatory pseudopod formation was abolished after the inhibition of either the activity of RhoA with C3 (□) or the activity of its effector kinase ROCK with Y-27632 (not shown). (*D*) The contour analysis of the shape change of the activated cell during the stimulation of pseudopod growth showed that the dominant shape change was the increase of the pseudopod length. (*E*) The shape changes during the stimulation of pseudopod growth by the different chemoattractants used here were similar for all chemoattractants.

from the cell surface for a time interval of 700 s. It is seen from the figure that for 700 s the pseudopod extended and retracted its length 12 times, although in two occasions the retraction of the pseudopod was almost complete. This oscillatory pseudopod formation was most probably actively regulated. To determine the pathway regulating the oscillatory pseudopod extension, we blocked the activity of the signaling molecules from the PI3K-dependent and -independent pathways of pseudopod extension that we have identified earlier (Chodniewicz and Zhelev, 2003a). Interestingly, the blocking of either RhoA activity with C3 or the activation of its downstream effector kinase ROCK with Y-27632 abolished pseudopod retraction, which resulted in an initial pseudopod extension and maintaining of the extended pseudopod at its maximal length for the duration of chemoattractant delivery. The blocking of RhoA activity did not arrest F-actin polymerization after reaching the maximal pseudopod length, which was detected from the continuous reshaping of the pseudopod leading edge after the maximal pseudopod length was reached.

The steep chemoattractant gradient created by the micropipet assay provided an opportunity for testing the predictions of the current models for cytoskeleton F-actin polymerization in the lamella region. The paradigm for F-actin polymerization in the lamella region postulates the assembly of a group of molecules, including WASp or WAVE, Arp2/3, the small GTPases Rac and Cdc42, and phosphatidylinositol (4,5)-bisphosphate (PtdIns(3,4)P_2) and phosphatidylinositol (3,4,5)-triphosphate (PtdIns(3,4,5)P_3), into molecular complexes that govern F-actin polymerization in the interior of the plasma membrane (Pollard and Borisy, 2003; Ridley et al., 2003). This mechanism of F-actin polymerization restricts the newly polymerized F-actin to the vicinity of the plasma membrane. The creation of a steep chemoattractant gradient by the micropipet assay, which allowed the activation of GPCRs only in a small area on the plasma membrane was expected to induce F-actin polymerization in a localized region of the activated cell. Therefore, the increase of the pseudopod length was expected to be the dominant shape change. Indeed, the contour analysis of the

change of the cell shape during pseudopod extension showed that the increase of the pseudopod length was much larger than any other shape change (Fig. 3 *D*). The shape of the pseudopod region was independent of the used chemoattractant (Fig. 3 *E*), which confirmed the hypothesis that the micropipet assay induced cytoskeleton F-actin polymerization only in a localized region of the cell and allowed us to use the rate of pseudopod extension as a measure for the rate of the process controlling F-actin polymerization in the pseudopod region. The rate of pseudopod extension was determined from the measured pseudopod length verses time as shown in Fig. 3 *B*.

Dependence of the rate of pseudopod extension on chemoattractant concentration

The rates of pseudopod extension induced by the ligands of the five classical chemotactic receptors considered here were similar for the range of concentrations from 10^{-10} to 10^{-6} M (Fig. 4). All measured rates reached saturation at 10^{-7} M chemoattractant. It is not known how different chemoattractants contribute to the signaling of F-actin polymerization in the lamella region; however, the observed similar rates of pseudopod extension for the different chemoattractants provided the opportunity to test whether the action of the different GPCRs is synergistic and whether there was a common rate-liming process for pseudopod extension.

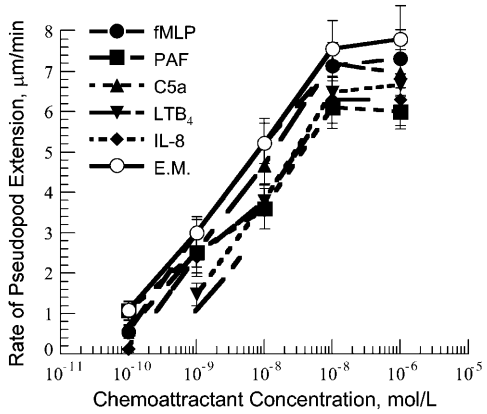

FIGURE 4 Rate of pseudopod extension verses chemoattractant concentration. The rate of pseudopod extension increased with the increase of the chemoattractant concentration for the range of concentrations from 10^{-10} to 10^{-7} M. The rate of pseudopod extension reached saturation above 10^{-7} M chemoattractant. The ● were for fMLP, the ■ were for PAF, the ▲ were for C5a, the ▼ were for LTB_4, the ♦ were for IL-8, and the ○ were for the equimolar mixture of all chemoattractants. The shown concentrations were the concentrations in the delivery pipet, and the distance between the leading edge of the pseudopod and the delivery pipet was 1 μm. Therefore, the actual chemoattractant concentrations at the leading edge of the pseudopod should be 30% smaller that the ones shown in the figure. The data points for pseudopod extension were expressed as the mean ± SD of at least 10 cells. The temperature was 25°C.

To determine whether the signaling of F-actin polymerization by different chemotactic receptors was synergistic, we induced pseudopod extension with a mixture of the five chemoattractants used here. In the mixture, the concentration of each chemoattractant was the same (equimolar mixture). For example, the equimolar mixture with 10^{-8} M total chemoattractant concentration contained 2×10^{-9} M of each fMLP, PAF, LTB_4, C5a, and IL-8. The rates of pseudopod extension induced by the equimolar mixture over the range of concentrations studied were somehow higher but similar to the same rates induced by individual chemoattractants. This showed that the action of the different GPCRs in the signaling of pseudopod extension was synergistic. Interestingly, the rates of pseudopod extension induced by the equimolar mixtures with 10^{-7}-M and 10^{-6}-M total chemoattractant concentrations were similar to the rate induced with 10^{-7} M fMLP or C5a. Since the concentrations of the individual chemoattractants in the 10^{-7}-M and 10^{-6}-M mixtures increased over a range where the individual chemoattractants had not reached saturation, it suggests that there is a common rate-limiting mechanism for pseudopod extension independent of the type of the activated GPCRs.

Effect of wortmannin on the rate of pseudopod extension

Wortmannin blocks PI3K activity and allows the determining of the degree of utilization of the PI3K-dependent signaling during pseudopod extension. The incubation of the cells with 1 μM wortmannin, which was the saturating concentration of this inhibitor for pseudopod extension (Chodniewicz and Zhelev, 2003a), decreased the rate of pseudopod extension induced with IL-8 by 55% and the rate of pseudopod extension induced by all other used chemoattractants from 72% to 80% (Fig. 5). This showed that except for the chemokine receptors, the F-actin polymerization signaled by the classical chemotactic receptors was strongly dependent on PI3K activation, which suggested that the rate-limiting process of the PI3K-dependent signaling of F-actin polymerization may be the rate-limiting process of pseudopod extension.

DISCUSSION

The results presented here provide important insights for the polymerization of cytoskeleton F-actin induced by G-protein coupled chemotactic receptors. They show that local activation of GPCRs by presenting the cell to a steep chemoattractant gradient induced cytoskeleton F-actin polymerization in a local region of the cell. This resulted in the formation of a single pseudopod, where the most significant change was the increase of pseudopod length. The delivery of chemoattractant to the cell surface in a diffusion-limited regime allowed for the stimulation of pseudopod

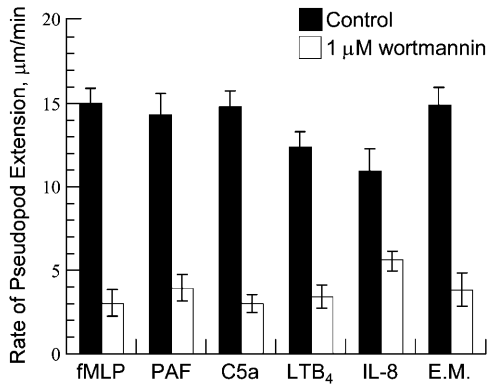

FIGURE 5 Effect of wortmannin on the rate of pseudopod extension. The incubation of the cells with 1 μM wortmannin for 15 min before the stimulation with chemoattractant decreased significantly the rate of pseudopod extension induced with fMLP (80% decrease), PAF (73% decrease), LTB_4 (72% decrease), and C5a (80% decrease). The rate of pseudopod extension was decreased only by 55% when the cells were stimulated with IL-8. The data points for pseudopod extension were expressed as the mean $\pm$ SD of at least eight cells. The temperature was 37°C.

extension by a constant concentration of chemoattractant and provided the opportunity to study the dependence of pseudopod extension on chemoattractant concentration. The finding that different chemoattractants induce pseudopod extension with similar rates is very interesting, because it suggests that the neutrophil has adjusted the expression of its chemotactic receptors with the affinity of binding of these receptors to their most common ligands and their ability to activate G-proteins to induce similar polymerization of cytoskeleton F-actin. This is in contrast to the ability of the same receptors to induce degranulation, superoxide production, or integrin activation (Nick et al., 1997; Berger et al., 2002; Haribabu et al., 2000). Therefore, the hierarchical response of the crawling neutrophils in complex chemoattractant environments (Heit et al., 2002; Foxman et al., 1999), such as the human body (Luster, 1998), is not a result of a differential capacity of the chemotactic receptors to induce F-actin polymerization. Other factors such as bound adhesion receptors (Willeke et al., 2000) or growth factor receptors (Chodniewicz and Zhelev, 2003b) most probably play a pivotal role in the modulation of the chemotaxis induced by chemotactic receptors in complex chemoattractant environments.

The existence of a rate-limiting process for pseudopod extension suggests that pseudopod extension is limited by the enzymatic reactions involved in the pathways of F-actin polymerization. The strong dependence of F-actin polymerization induced with fMLP, LTB_4, PAF, and C5a on PI3K activity suggests that this pathway could provide the rate-limiting process for pseudopod extension. Our earlier finding that the PI3K pathway is represented by a cascade of enzymes including protein kinase C (PKC) and Akt/protein kinase B (PKB) (Chodniewicz and Zhelev, 2003a) suggests that pseudopod extension may be limited by the slowest enzymatic reaction in the pathway. We have studied this possibility in more detail and have found that, indeed, the rate of pseudopod extension was limited by the enzymatic activity of its signaling reactions (Chodniewicz et al., 2004).

The discovery of the oscillatory pseudopod extension is intriguing. Crawling neutrophils change their direction of movement by either following the change of the direction of the chemoattractant gradient or by repolarizing in the new gradient (Zigmond et al., 1981). Most of the cells (60%) follow the change of the stimulus direction; however, a significant fraction of the cells (30%) repolarize in the direction of the newly established gradient (Zigmond et al., 1981). The studying of the mechanism of establishing cell polarity using HL-60 cells differentiated into neutrophil-like cells showed that RhoA and ROCK play pivotal roles in signaling of polarity (Xu et al., 2003). In view of this finding, and our finding that the oscillatory pseudopod formation was abolished after blocking RhoA or ROCK activity, we propose that the role of the oscillatory pseudopod formation is to provide means for the crawling cell to change its direction of crawling via repolarization in a newly established gradient.

This work was supported by grant HL57629 to D.Z. from the National Institutes of Health. D.C. was a recipient of a fellowship from the National Institutes of Health Research Training Grant GM08555. Blood drawing was supported by grant M01-RR-30 from the National Institutes of Health to the General Clinical Research Centers Program at Duke University.

REFERENCES

Alteraifi, A. M., and D. V. Zhelev. 1997. Transient increase of free cytosolic calcium during neutrophil motility responses. *J. Cell Sci.* 110:1967–1977.

Berger, M., S. Budhu, E. Lu, Y. Li, D. Loike, S. C. Silverstein, and J. D. Loike. 2002. Different Gi-coupled chemoattractant receptors signal qualitatively different functions in human neutrophils. *J. Leukoc. Biol.* 71:798–806.

Chodniewicz, D., A. M. Alteraifi, and D. V. Zhelev. 2004. Experimental evidence for the limiting role of enzymatic reactions in chemoattractant-induced pseudopod extension in human neutrophils. *J. Biol. Chem.* 279:24460–24466.

Chodniewicz, D., and D. V. Zhelev. 2003a. Chemoattractant receptor stimulated F-actin polymerization in the human neutrophil is signaled by two distinct pathways. *Blood.* 101:1181–1184.

Chodniewicz, D., and D. V. Zhelev. 2003b. Novel pathways of F-actin polymerization in the human neutrophil. *Blood.* 102:2251–2258.

Cottler-Fox, M. H., T. Lapidot, I. Petit, O. Kollet, J. F. DiPersio, D. Link, and S. Devine. 2003. Stem cell mobilization. *Hematology.* 419–437.

Davies, S. P., H. Reedy, M. Caivano, and P. Cohen. 2000. Specificity and mechanism of action of some commonly used protein kinase inhibitors. *Biochem. J.* 351:95–105.

Foxman, E. F., E. J. Kunkel, and E. C. Butcher. 1999. Integrating conflicting chemotactic signals: the role of memory in leukocyte navigation. *J. Cell Biol.* 147:577–588.

Haribabu, B., R. M. Richardson, M. W. Verghese, A. J. Barr, D. V. Zhelev, and R. Snyderman. 2000. Function and regulation of chemoattractant receptors. *Immunol. Res.* 22:271–279.

Haribabu, B., D. V. Zhelev, B. C. Pridgen, R. M. Richardson, H. Ali, and R. Snyderman. 1999. Chemoattractant receptors activate distinct pathways for chemotaxis and secretion. Role of G-protein usage. *J. Biol. Chem.* 274:37087–37092.

Heit, B., S. Tavener, E. Raharjo, and P. Kubes. 2002. An intracellular signaling hierarchy determines direction of migration in opposing gradients. *J. Cell Biol.* 159:91–102.

Juarez, J., and L. Bendall. 2004. SDF-1 and CXCR4 in normal and malignant hematopoiesis. *Histol. Histopathol.* 19:299–309.

Katanaev, V. L. 2001. Signal transduction in neutrophil chemotaxis. *Biochemistry.* 66:351–368.

Luster, A. D. 1998. Mechanisms of disease: chemokines-chemotactic cytokines that mediate inflammation. *N. Engl. J. Med.* 338:436–445.

Martin, C., P. C. E. Burton, G. Bridger, J. C. Gutierrez-Ramos, T. J. William, and S. M. Rankin. 2003. Chemokines acting via CXCR2 and CXCR4 control the release of neutrophils from the bone marrow and their return following senescence. *Immunity.* 19:583–593.

Moghe, P. V., R. D. Nelson, and R. T. Tranquillo. 1995. Cytokine-stimulated chemotaxis of human neutrophils in a 3-D conjoined fibrin gel assay. *J. Immunol. Methods.* 180:193–211.

Nick, J. A., N. J. Avdi, S. K. Young, C. Knall, P. Gerwins, G. L. Johnson, and G. S. Worthen. 1997. Common and distinct intracellular signaling pathways in human neutrophils utilized by platelet activating factor and FMLP. *J. Clin. Invest.* 99:975–986.

Niggli, V., and H. Keller. 1997. The phosphatidylinositol 3-kinase inhibitor wortmannin markedly reduces chemotactic peptide-induced locomotion and increases in cytoskeletal actin in human neutrophils. *Eur. J. Pharmacol.* 335:43–52.

Papayannopoulou, T. 2004. Current mechanistic scenarios in hematopoietic stem/progenitor cell mobilization. *Blood.* 103:1580–1585.

Pollard, T. D., L. Blanchoin, and R. D. Mullins. 2000. Molecular mechanisms controlling actin filament dynamics in nonmuscle cells. *Annu. Rev. Biophys. Biomol. Struct.* 29:545–576.

Pollard, T. D., and G. G. Borisy. 2003. Cellular motility driven by assembly and disassembly of actin filaments. *Cell.* 112:453–465.

Pruijt, J. F. M., P. Verzaal, R. van Os, E.-J. F. M. de Kruijf, M. L. J. van Schie, A. Mantovani, A. Vecchi, I. J. D. Lindley, R. Willemze, S. Starckx, G. Opdenakker, and W. E. Fibbe. 2002. Neutrophils are indispensable for hematopoietic stem cell mobilization induced by interleukin-8 in mice. *Proc. Natl. Acad. Sci. USA.* 99:6228–6233.

Ridley, A. J., M. A. Schwartz, K. Burridge, R. A. Firtel, M. H. Ginsberg, G. Borisy, J. T. Parsons, and A. R. Horwitz. 2003. Cell migration: integrating signals from front to back. *Science.* 302:1704–1709.

Stickle, D. F., D. A. Lauffenburger, and S. H. Zigmond. 1984. Measurement of chemoattractant concentration profiles and diffusion coefficient in agarose. *J. Immunol. Methods.* 70:65–74.

Stoyanova, S., G. Bulgarelli-Veva, C. Kirsch, T. Hanck, R. Klinger, R. Wetzker, and M. P. Wymann. 1997. Lipid kinase and protein kinase activities of G-protein-coupled phosphoinositide 3-kinase γ: structure–activity analysis and interactions with wortmannin. *Biochem. J.* 324: 489–495.

Tarlowe, M. H., K. B. Kannan, K. Itagaki, J. M. Adams, D. H. Livingston, and C. J. Hauser. 2003. Inflammatory chemoreceptor cross-talk suppresses leukotriene B4 receptor 1-mediated neutrophil calcium mobilization and chemotaxis after trauma. *J. Immunol.* 171:2066–2073.

Tessier, P. A., P. H. Naccache, I. Clark-Lewis, R. P. Gladue, K. S. Neote, and S. R. McColl. 1997. Chemokine networks in vivo: involvement of C–X-C and C–C chemokines in neutrophil extravasation in vivo in response to TNF-alpha. *J. Immunol.* 159:3595–3602.

Thelen, M., M. Wymann, and H. Langen. 1994. Wortmannin binds specifically to 1-phosphatidylinositol 3-kinase while inhibiting guanine nucleotide-binding protein-coupled receptor signaling in neutrophil leukocytes. *Proc. Natl. Acad. Sci. USA.* 91:4960–4964.

Willeke, T., S. Behrens, K. Scharffetter-Kochanek, P. Gaehtgens, and B. Walzog. 2000. β2 integrin (CD11/CD18)-mediated signaling involves tyrosine phosphorylation of c-Cbl in human neutrophils. *J. Leukoc. Biol.* 68:284–292.

Wymann, M. P., G. Bulgarelli-Leva, M. J. Zvelebil, L. Pirola, B. Vanhaesebroeck, M. D. Waterfield, and G. Panayotou. 1996. Wortmannin inactivates phosphoinositide 3-kinase by covalent modification of Lys-802, a residue involved in the phosphate transfer reaction. *Mol. Cell. Biol.* 16:1722–1733.

Xu, J., F. Wang, A. V. Keymeulen, P. Herzmark, A. Straight, K. Kelly, Y. Takuwa, N. Sugimoto, T. Mitchison, and H. R. Bourne. 2003. Divergent signals and cytoskeletal assemblies regulate self-organizing polarity in neutrophils. *Cell.* 114:201–214.

Zhang, X. W., Q. Liu, Y. Wang, and H. Thorlacius. 2001. CXC chemokines, MIP-2 and KC, induce P selectin-dependent neutrophil rolling and extravascular migration in vivo. *Br. J. Pharmacol.* 133: 413–421.

Zhelev, D. V., A. M. Alteraifi, and R. M. Hochmuth. 1996. F-actin network formation in tethers and in pseudopods stimulated by chemoattractant. *Cell Motil. Cytoskeleton.* 35:331–344.

Zhelev, D. V., and D. Needham. 1993. Tension-stabilized pores in giant vesicles: determination of pore size and pore line tension. *Biochim. Biophys. Acta.* 1147:89–104.

Zigmond, S. H., H. I. Levitsky, and B. J. Kreel. 1981. Cell polarity: an examination of its behavioral expression and its consequences for polymorphonuclear leucocyte chemotaxis. *J. Cell Biol.* 89:585–592.